9.3. Snímače sily

- **deformačné členy + snímanie :**
  - mech. napätia - tenzometre
  - zmeny polohy - malé výchyľky [mm, um]
- **piezoelektrické** - nevhodné pre statické merania
- **kapacitné**
- **magnetoanizotropné**
- **zmena elektrického odporu**

9.3. Snímače sily - aplikácie

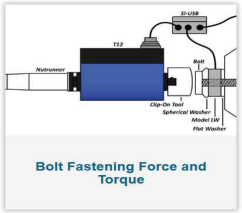

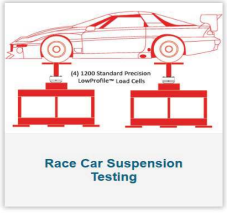

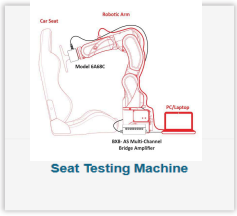

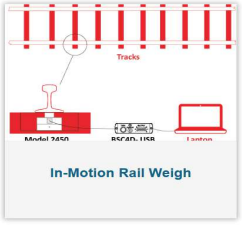

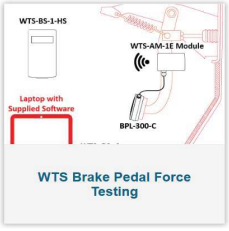

9.3. Snímače sily - aplikácie

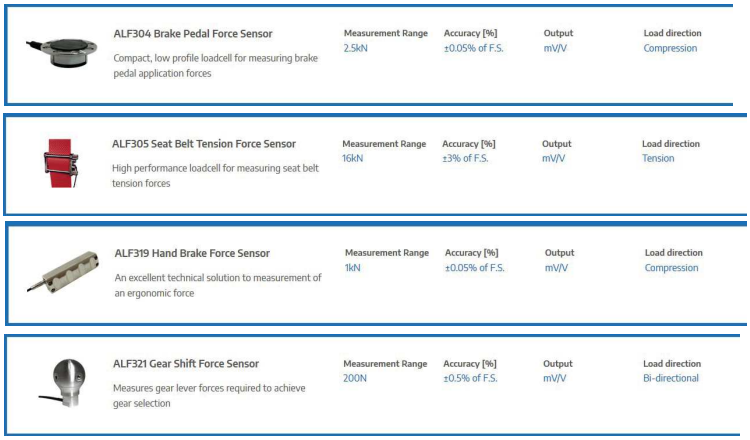

9.3. Snímače sily - aplikácie

Force-sensing: A third dimension in automotive touch controls

Synaptics demonstration of a steering wheel touchpad with force sensing and haptics.

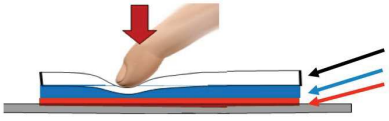

- Tx and Rx channels for 2D touch sensing
- Compressible elastomer
- Pressure sensing Rx channels

9.3. Snímače sily

Deformačné členy

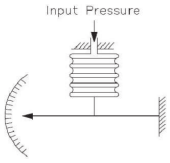

Menia pôsobiacu silu na inú veličinu

- **nosníky** → deformácia, tenzometre
- **pružiny** → zmena polohy , snímač polohy (indukčný, fotoelektrický)
- **pružné podložky** → zmena polohy

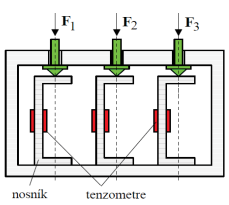

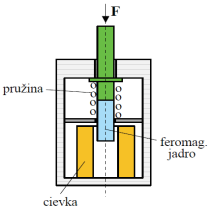

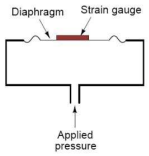

9.3.1 Deformačné členy

Tenzometer – Strain Gauge

Definition of strain, ε

$$\varepsilon = \frac{\Delta L}{L}$$

Tenzometre

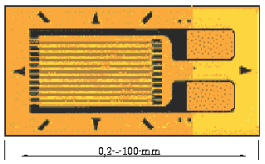

a

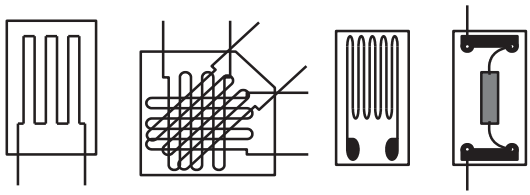

Tenzometre

Tab.1 Prehľad vlastností nalepených tenzometrov

Tenzometre	Fóliové		Polovodičový
Typ	KFC-2-D1-23 (R_{xC})	KFC-5-350-C1-23 (R_{xA}, R_{xB}, R_{xE})	KSP-2-E3 (R_{xD})
Odpor R [Ω]	119.9±0.4	350±0.6	110±2%
Súčiniteľ deformačnej citlivosti K	2.11	2.1±1%	124±3%
Teplotný súčiniteľ deformačnej citlivosti $\alpha_{k0,u}$ [1/°C]	≈ 0	≈ 0	0.14%
Teplotný súčiniteľ elektrického odporu $\alpha_{R0,\upsilon}$ [μm/m//°C, tj. ε/°C]	1.8	1.8	13.8
Súčiniteľ teplotnej rozťažnosti materiálu tenzometra α_S[μm/m//°C]	≈ 0	≈ 0	7÷22
Výrobca	Kyowa Tokyo	Kyowa Tokyo	Kyowa Tokyo
Max. relatívne predĺženie ε [μm/m]	±3000	±3000	±2000
Dĺžka aktívnej mriežky [mm]	2	5	2
Poznámka	tepelná kompenzácia pre namáhaný material-hlinik(23 μm/m//°C)	tepelná kompenzácia pre namáhaný material-hlinik(23 μm/m//°C)	

Membrane type gauges: typical pressure sensor

MEMS Tenzometre

Implantable strain gauge

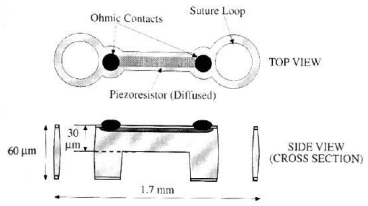

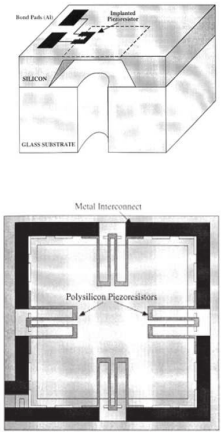

Tenzometre

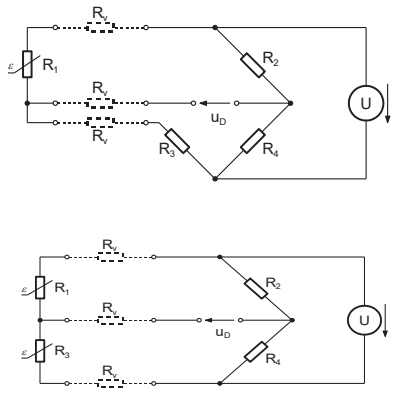

Tenzometre

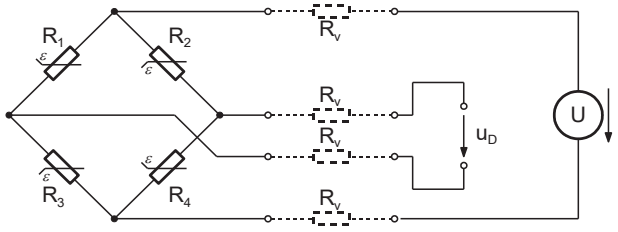

Využitie tenzometrov

Sila

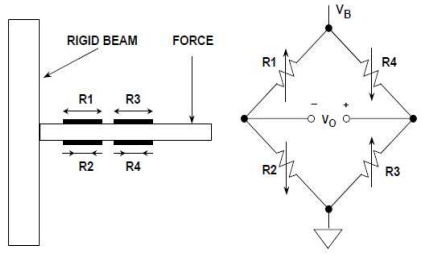

Figure 3.83: A beam force sensor using a strain gage bridge

Využitie tenzometrov

Váženie

9.3. Snímače sily

Kapacitné snímače

Table 5.1 Fundamental types of capacitive force transducers (CFTs)

Type	Flat Parallel	Cylindrical Coaxial	Spherical Concentric
Layout	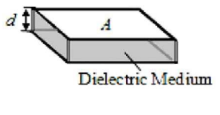	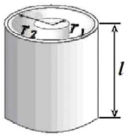	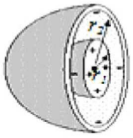
Formula	$C = \frac{\varepsilon_r \cdot \varepsilon_0 \cdot A}{d}$	$C = \frac{2\pi\varepsilon_r \cdot \varepsilon_0 \cdot l}{\ln(r_2/r_1)}$	$C = \frac{4\pi\varepsilon_r \cdot \varepsilon_0 \cdot r_1 \cdot r_2}{r_2 - r_1}$

9.3. Snímače sily

PPS - TactArray

Kapacitné snímače

CTA's are flexible and can be molded over complex shapes like a head

Sensor Characteristics & Performance

Full Scale Range	2-80 psi
Thickness	< 1 mm (< 0.04 in)
Signal-to-Noise (SNR)	> 500:1
Minimum Sensitivity	10 Pa (0.0015 psi)
Linearity	99.8%
Gain Non-Repeatability	0.35%
Weight	~ 1.5 lbs (650 g)

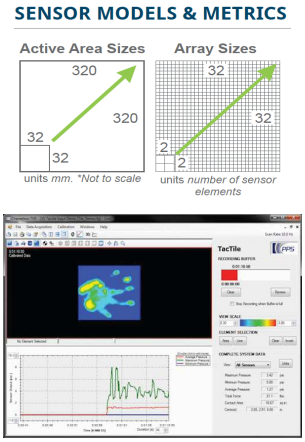

9.3. Snímače sily

Piezoelektrické snímače

- **využívajú vznik náboja pri pôsobení sily** (U = Q/C)
- **smer polarizácie** - smer citlivosti
- **statické merania**
  - náboj po čase "zmizne"
- **materiál – piezokeramika**

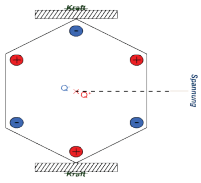

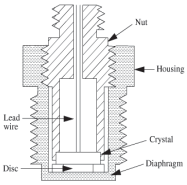

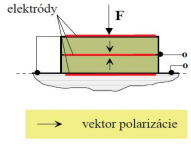

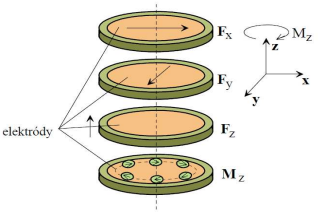

9.3. Snímače ~~sily~~ zrýchlenia

Piezoelektrické snímače

- **teliesko so známou hmotnosťou** *m*, **pri pôsobení sily**
  F = m.a
  → snímač zrýchlenia
- meranie vibrácií, diagnostika, monitoring

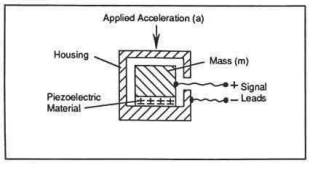

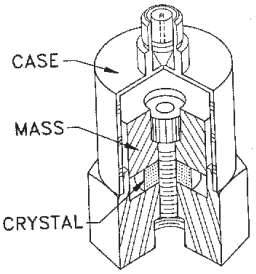

9.3. Snímače sily
Piezoelektrické snímače

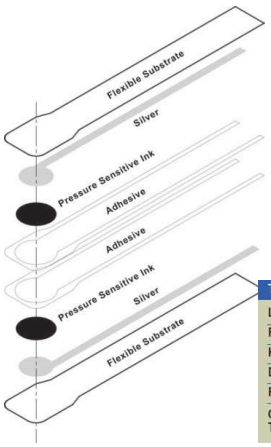

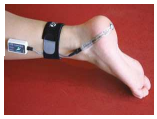

Typical Performance	
Linearity (Error)	< ±3%
Repeatability	< ± 2.5% of Full Scale
Hysteresis	< 4.5% of Full Scale
Drift	< 5% per Logarithmic Time Scale
Response Time	< 5µsec
Operating Temperature	15°F - 140°F (-9°C - 60°C)

9.3. Snímače sily
Magnetoanizotropné snímače

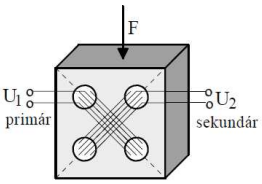

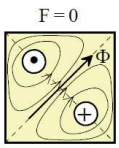

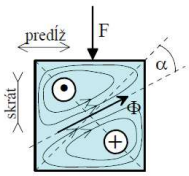

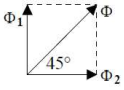

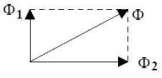

hranol z feromagn. materiálu (permalloy) + dve vinutia prevlečené cez otvory s navzájom ⊥ osami, tvoria transformátor

bez pôsobenia sily sekundár neviaže žiadny mag. tok, U2 je nulové

pri silovej deformácii nastanú tieto javy (obecne) :

ťah → +σ (predĺženie) → μ_r stúpa → mag tok Φ stúpa
tlak → - σ (skrátenie) → μ_r klesá → mag tok Φ klesá

9.3. Snímače sily
Magnetoanizotropné snímače

snímač pre F = 5000 kN
(fy ASEA Švédsko)

- linearita, presnosť 0,5 %
- hysteréza 0,2 %
- stlačenie 0,05 mm
- preťaženie 200 %
- rozsah teplôt +20 ÷ +80 °C
- napájacia f 50, 60, 400 Hz

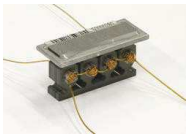

9.3. Snímače sily
Zmena elektrického odporu

- **vodivá guma**
- **plastické hmoty (polyuretán)**

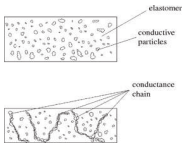

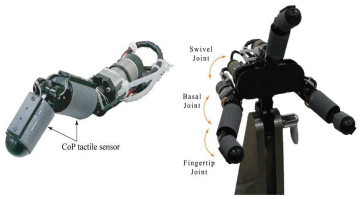

Materiály vykazujú zmenu odporu pri stláčaní
Miera stlačenia úmerná sile (niekedy pomocná pružina)

Poznámka: Materiály majú značnú časovú a teplotnú chybu

9.3.2 Rezonančné snímače sily
Detekcia DNA

Piezoelectric Disk Resonators for Direct Molecular Sensing

- ❑ Rotational mode disk resonators are demonstrated as direct real-time bio-molecule monitors
- ❑ Exposure to 1.0 mM MCH in aqueous solution
- ❑ Saturation is reached after 1hr

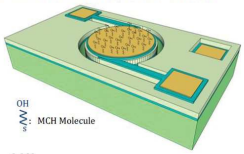

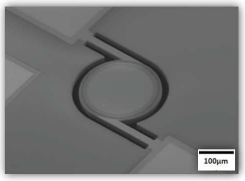

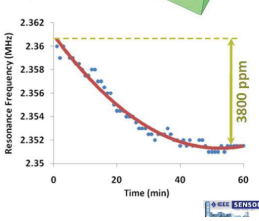

Experiments and Results

DNA Detection Mechanism

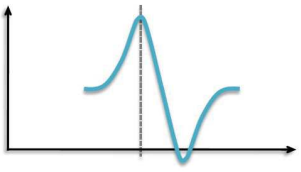

Blank gold surface
(I) Treatment with HS-ssDNA (2.0 µM/1.0 M KH_2PO_4, PH 4.2)
(II) Exposure to 1.0 mM Mercapto-Hexanol in aqueous solution
(III) Hybridization with Complementary DNA Solution (1.0 µM/1.0 M NaCl Tris-HCl 1.0 mM EDTA)

Experiments and Results

DNA Detection Mechanism

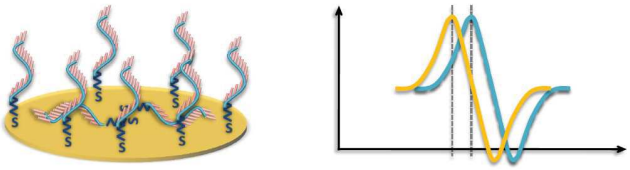

Blank gold surface
(I) Treatment with HS-ssDNA (2.0 μM/1.0 M KH_2PO_4, PH 4.2)
(II) Exposure to 1.0 mM Mercapto-Hexanol in aqueous solution
(III) Hybridization with Complementary DNA Solution (1.0 μM/1.0 M NaCl Tris-HCl 1.0 mM EDTA)

Experiments and Results

DNA Detection Mechanism

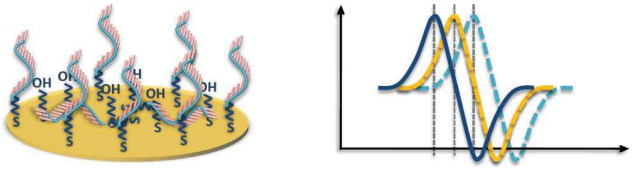

Blank gold surface
(I) Treatment with HS-ssDNA (2.0 μM/1.0 M KH_2PO_4, PH 4.2)
(II) Exposure to 1.0 mM Mercapto-Hexanol in aqueous solution
(III) Hybridization with Complementary DNA Solution (1.0 μM/1.0 M NaCl Tris-HCl 1.0 mM EDTA)

9.4. Snímače zrýchlenia

$$\mathbf{a} = \lim_{\Delta t \to 0} \frac{\Delta \mathbf{v}}{\Delta t} = \frac{\mathrm{d}\mathbf{v}}{\mathrm{d}t}$$

SI jednotka je **m/s²**

$$F = m \cdot a$$

$$F = k \cdot \Delta x$$

$$a = \frac{k}{m} \Delta x$$

$$a_g = \varkappa \frac{M}{R^2}$$

9,764 – 9,834 m/s²

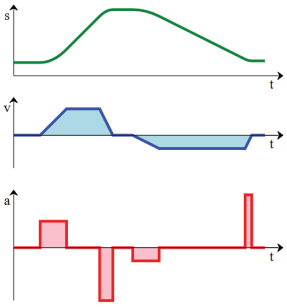

Zdola nahor:
časový priebeh zrýchlenia *a(t)*, integrál zrýchlenia je rýchlosť *v(t)*, a integrovaním rýchlosti získame priebeh dráhy *s(t)*.

9.4. Snímače zrýchlenia

- Zrýchlenie $a = dv / dt$
- Newtonov zákon $F = m.a$

Pri známej hmotnosti telesa *m* je sila *F* merítkom zrýchlenia *a*.

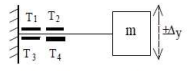

Obr. 3.77 Tenzometrický snímač zrychlení

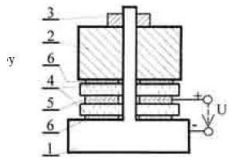

Obr. 3.78b Piezoelektrický tlakový snímač zrychlení

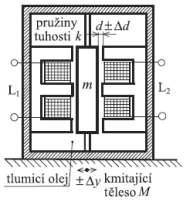

Obr. 3.79 Indukčnostní snímač zrychlení

9.4. Snímače zrýchlenia – akcelerometre

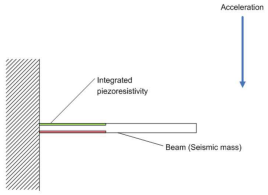

Piezorezistívne

Piezoelektrické

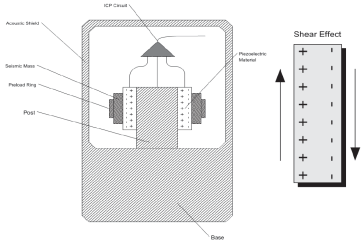

9. 4. Meranie zrýchlenia

Applications of MEMS Accelerometers

Industrial
- Platform stabilization
- Oil drilling orientation
- Robotic telepresence

Automotive
- Airbag deployment
- Rollover, anti-skid control

Consumer
- Interactive gaming
- Free-fall detection
- Camera stabilization
- Indoor navigation

Military
- Aircraft flight control
- Dead-reckoning

Georgia Tech Qualtré IEEE SENSORS 2013

Electromechanical Transduction

- Displacement has to be converted into electrical signal
- Most common sensing mechanisms:

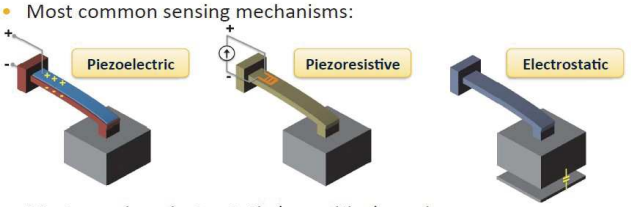

- Most popular: electrostatic (capacitive) sensing

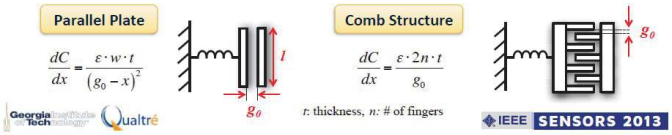

Georgia Tech Qualtré IEEE SENSORS 2013

MEMS akcelerometer

ADXL202: ±2 g Dual Axis Accelerometer

Features
- X and Y Axis on a single chip = Small size and lower cost
- 250uA per Axis = Low power battery operation
- 3.0V to 5.0V Operation = Low power battery operation
- Surface mount package = Small size and ease of use
- High resolution PWM converter = Direct interface to micro (No A/D)
- iMEMS = Low cost AND high performance

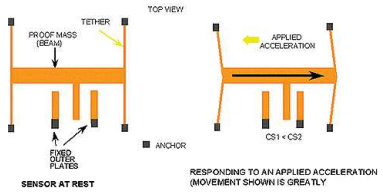

MEMS akcelerometer

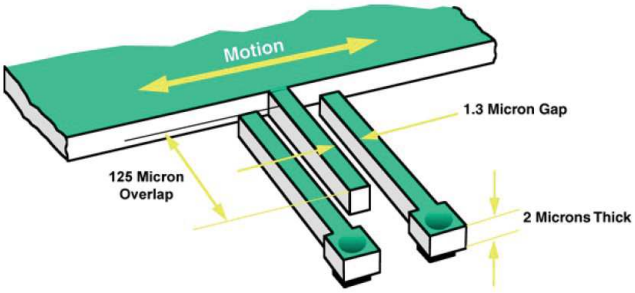

MEMS akcelerometer

ADXL 202: Micromachined Beam

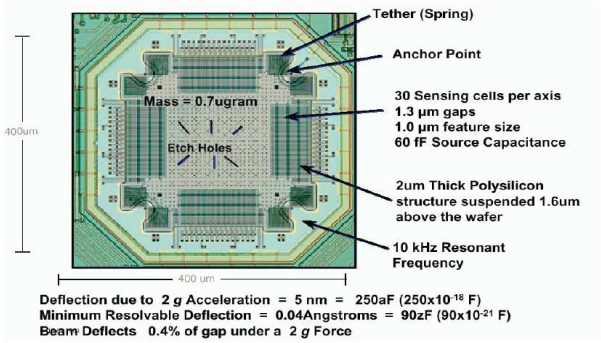

Deflection due to 2 *g* Acceleration = 5 nm = 250aF (250×10^{-18} F)
Minimum Resolvable Deflection = 0.04Angstroms = 90zF (90×10^{-21} F)
Beam Deflects 0.4% of gap under a 2 *g* Force

MEMS akcelerometer

ADXL 202: acceleration sensor

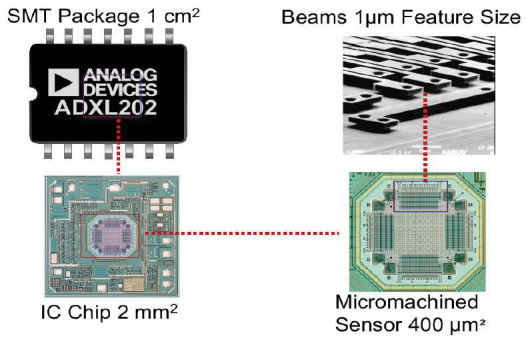

MEMS akcelerometer

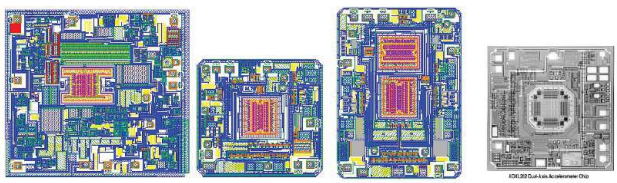

XL50
First Airbag Sensor
50g Analog Output
1993 Saab

XL150
2nd Gen Airbag
50g Analog Out

XL250
2nd Gen Airbag
2 Axis 50g Analog out
Side Impact

XL202
2 Axis 2g
Digital Output
1.2X XL150

Evolution of MEMS Accelerometers

- Analog Devices Accelerometer (Automotive)

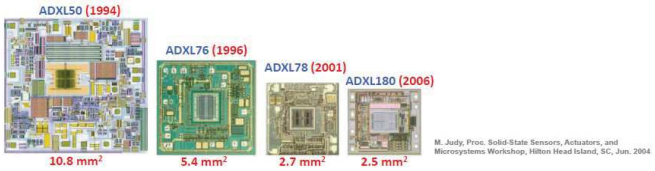

- STMicroelectronics Accelerometer (Consumer)

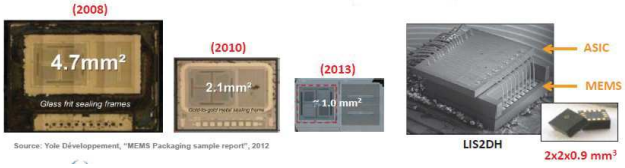

MEMS Capacitive Accelerometers

- Conventional MEMS accelerometer architecture

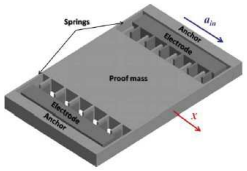

Lumped-Element Model

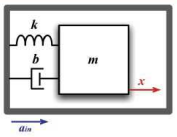

Steady state response:

$$m a_{in} = -k x$$

$$\frac{x}{a_{in}} = -\frac{m}{k}$$

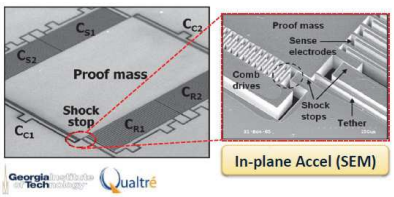

In-plane Accel (SEM)

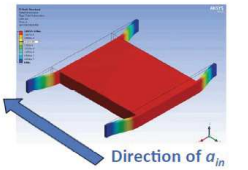

IEEE SENSORS 2013

MEMS akcelerometer

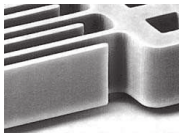

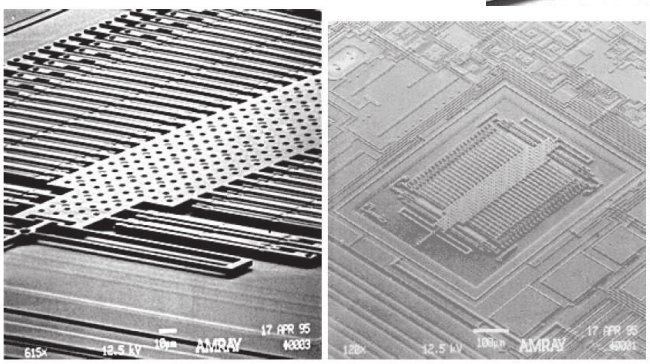

MEMS akcelerometer

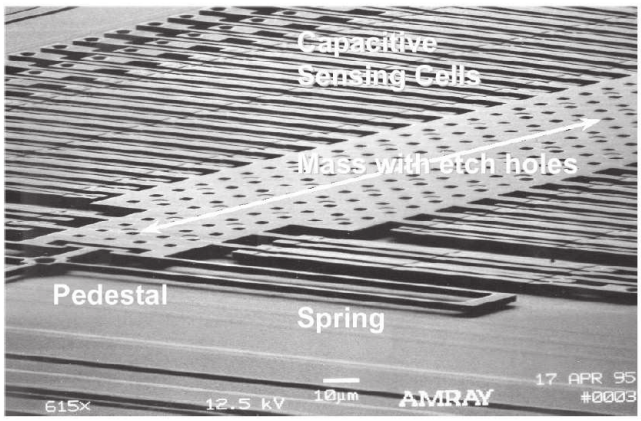

MEMS akcelerometer

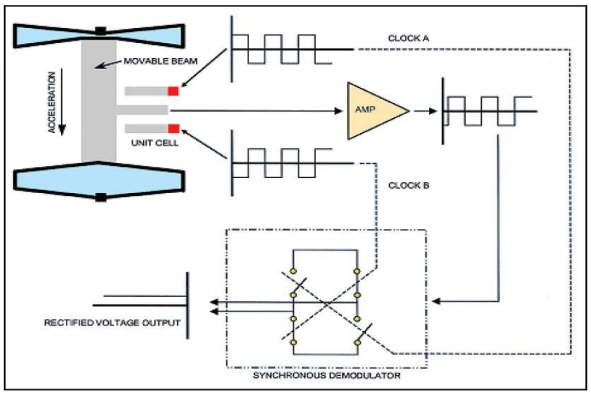

MEMS akcelerometer

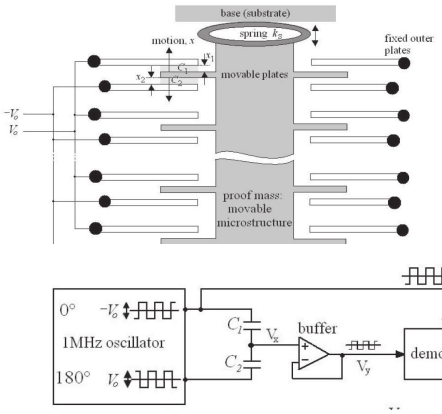

$$C_1 = \epsilon_A \frac{1}{x_1} = \epsilon_A \frac{1}{d+x} = C_0 - \Delta C,$$

$C_t = C_{11} \parallel C_{12} \parallel \ldots \parallel C_{1n}$

$$x \approx \frac{d^2}{\epsilon_A} \Delta C = d \frac{\Delta C}{C_0}$$

C_1 a C_2 tvoria impedančný napäťový delič

MEMS akcelerometer

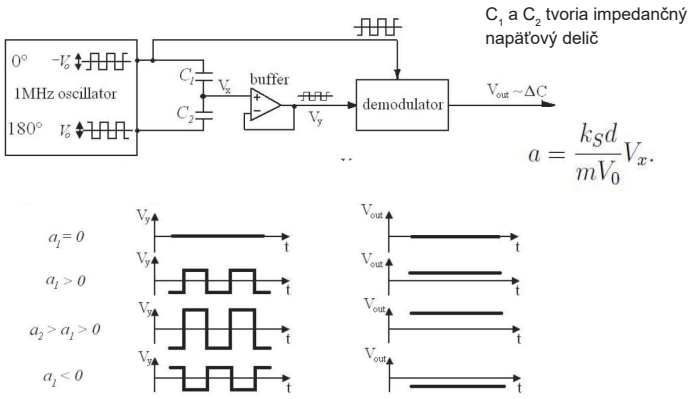

C_1 a C_2 tvoria impedančný napäťový delič

$$a = \frac{k_S d}{m V_0} V_x.$$

MEMS akcelerometer

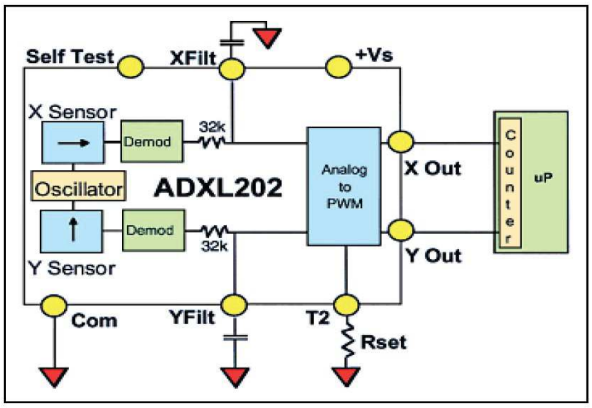

MEMS akcelerometer

- Piezoresistive MEMS accelerometer
  - Operating Principle: a proof mass attached to a silicon housing through a short flexural element. The implantation of a piezoresistive material on the upper surface of the flexural element. The strain experienced by a piezoresistive material causes a position change of its internal atoms, resulting in the change of its electrical resistance
  - low-noise property at high frequencies

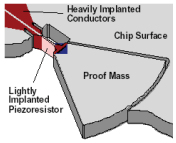

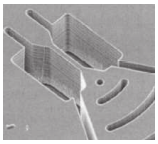

Courtesy of JP Lynch, U Mich.

MEMS MX2125 hot bubble

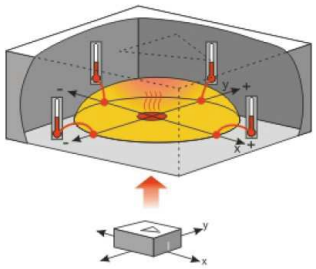

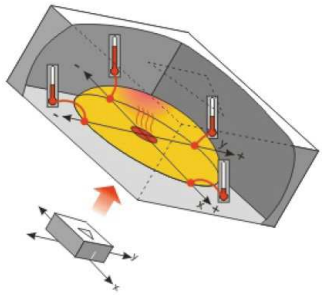

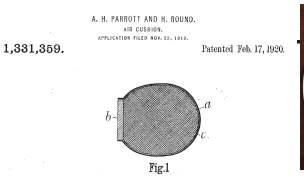

United States patent submitted in 1919 by two dentists, **Harold Round** & **Arthur Parrott** of Birmingham, England

John Hetrick's original airbag design from 1953

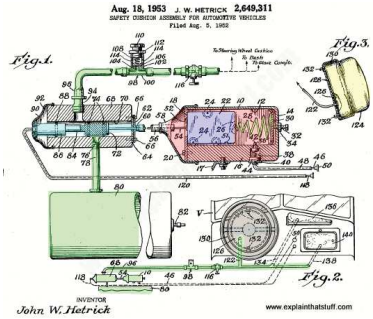

Allen K. Breed (1927–2000), who developed a variety of different ways of triggering the explosion of gas inside an airbag just before the impact of a crash.

Bellis, Mary. "The History of Airbags." ThoughtCo, Feb. 11, 2020, thoughtco.com/history-of-airbags-1991232.

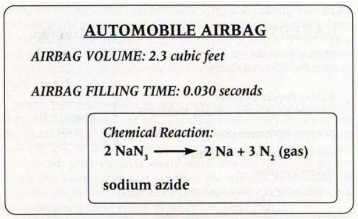

Gas-Generator Reaction	Reactants	Products
First Reaction (Triggered by Sensor)	NaN_3	Na N_2 (g)
Second Reaction.	Na KNO_3	K_2O Na_2O N_2 (g)
Final Reaction.	K_2O Na_2O SiO_2	alkaline silicate (glass)

Figure 11.

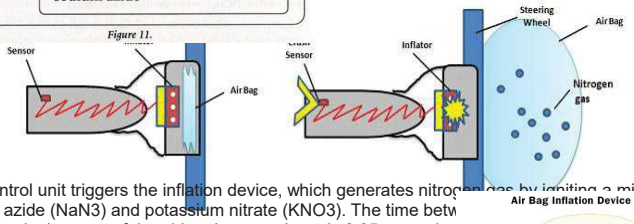

This control unit triggers the inflation device, which generates nitrogen gas by igniting a mixture of sodium azide (NaN3) and potassium nitrate (KNO3). The time betw) complete deployment of the airbag is approximately 0.05 seconds. mph, which itself can be harmful in certain cases.

Most systems use a weight sensor in the front passenger seat to d . If it is not, the passenger airbag will not deploy. The weight sensor children and adults who may be occupying the seat.

https://cecas.clemson.edu/cvel/auto/systems/airbag_deployment.
http://allaboutairbagdeployment.weebly.com/part-three.html

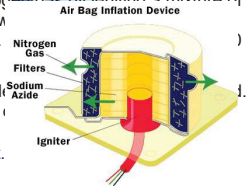

Mechanické

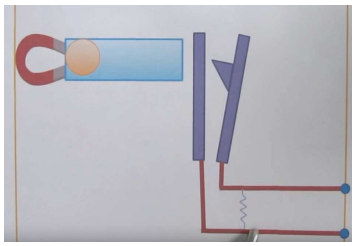

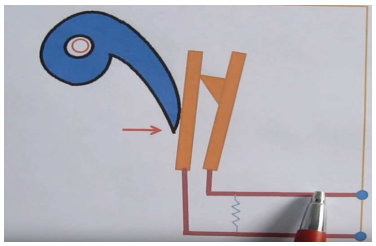

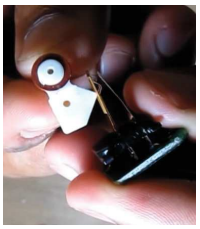

Mechanické

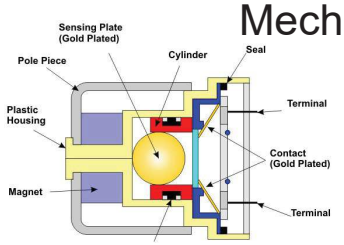

Figure 1. Structural components to an Inertia sensor. Source: Duffy, J.E. (2001). I-Car Professional Automotive Collision Repair. New York: Delmar, a division of Thomas Learning.

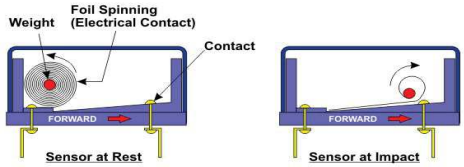

Figure 2. Functional principle to a typical roller type airbag sensor. Source: Erjavec, J. (2010). Automotive Technology: A Systems Approach. New York: Delmar, Cengage Learning.

https://www.azosensors.com/article.aspx?ArticleID=40

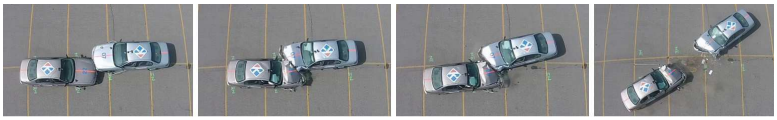

the airbag deployment decision depends upon acceleration and jerk

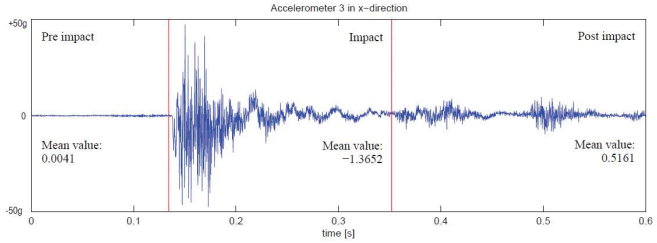

Airbagy – deploy or not deploy?

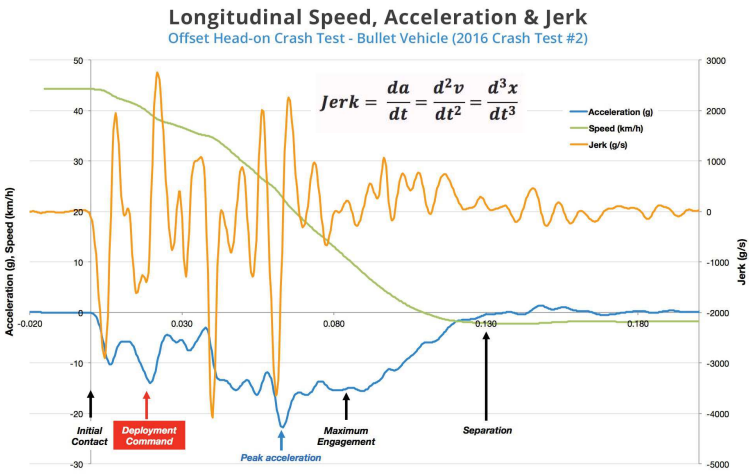

Gyroskop

Leon Foucault

experimental apparatus for Earth's rotation observation by joining two Greek roots: *gyros* - rotation and *skopeein* - to see

Foucaultovo kyvadlo 1851 Panteon, Paris

Gyroscope invented by Léon Foucault in 1852. Replica built by Dumoulin-Froment for the Exposition universelle in 1867. National Conservatory of Arts and Crafts museum, Paris.

Source: https://en.wikipedia.org/wiki/Gyroscope#/media/File:Foucault's_gyros

Odbočka (1851)

Foucaultovo kyvadlo

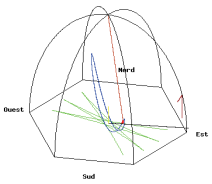

$$\omega = 360^\circ \sin\varphi \,/\mathrm{day},$$

where φ is latitude,
m = 28 kg,
L = 67 m $\quad T = 2\pi\sqrt{\frac{l}{g}} = 16.5$ s

1 otáčka $\frac{23h56'}{\sin\phi}$ = 31.8 hours

t.j. 11.3° / hod

; ϕ = 48°52' N

Foucault's pendulum in the Panthéon, Paris

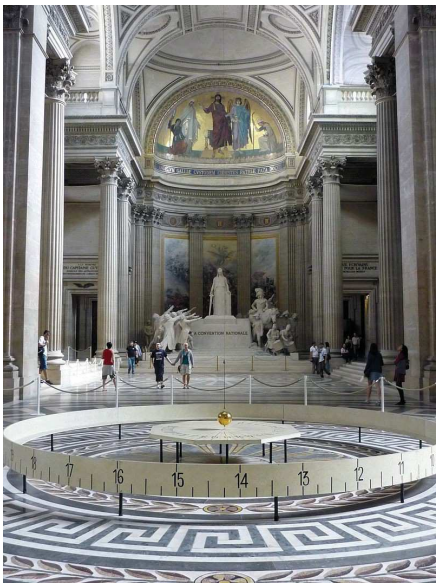

Odbočka 2

Kardanov záves - Gimbal

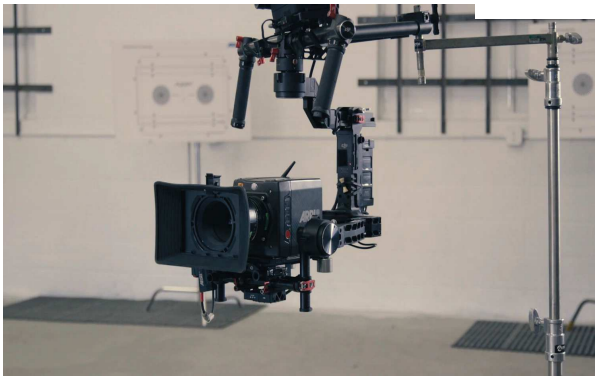

9. 4. Meranie zrýchlenia

Aplikácie gyroskopov

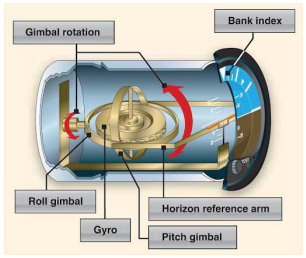

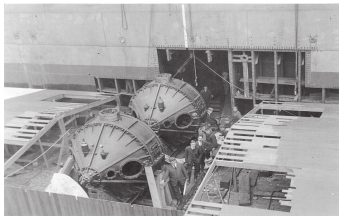

1

What is a Gyroscope?

- Sensor that measures the angle or rate of rotation

Spinning Gyroscopes

Conservation of angular momentum

Optical Gyroscopes

Sagnac Effect

Vibratory Gyroscopes

Coriolis Effect

MEMS

NMR Gyroscopes

Larmor Precession Rate

IEEE SENSORS 2013

9. 4. Meranie zrýchlenia

MEMS gyroskopy

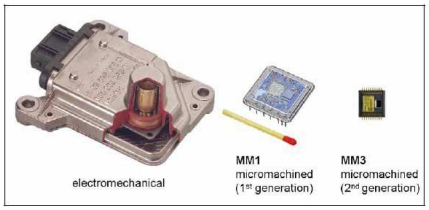

Generations of gyroscope sensors for the Electronic Stability Program ESP®.

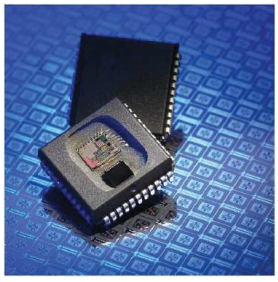

Gyroscope sensor for rollover detection, by Bosch.

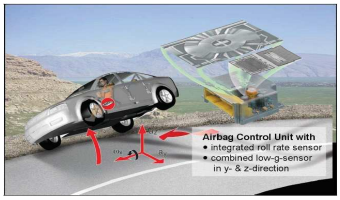

9. 4. Meranie zrýchlenia

MEMS gyroskopy

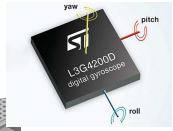

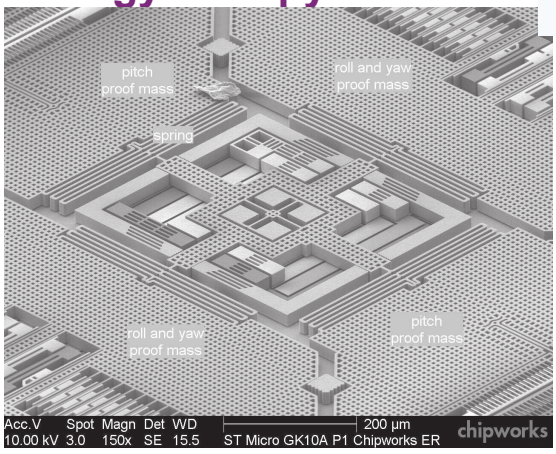

Evolution of MEMS Gyroscopes

- STMicroelectronics 3-Axis Gyroscope (Consumer)

Source: Yole Développement, "STMicro L3G3250A Reverse costing", 2012

- Invensense 3-Axis Gyroscope (Commercial)

Product	IDG-1000	IDG-600	IXZ-600	MPU-3000	
MP Date	2006	2008	2009	2010	
Gyro Axes	X/Y	X/Y	X/Z	X/Y/Z	
Package	6x6x1.4 QFN	5x4x1.2 QFN	5x4x1.2 QFN	4x4x0.9 QFN	mm³
Die Size	12.2	7.4	7.4	6.7	mm²
MEMS Area	4.1	2.8	2.8	2.9	mm²
CMOS technology	0.5um	0.35um	0.35um	0.18um	
Output	Analog	Analog	Analog	Digital	

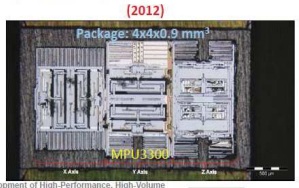

Source: Seeger, et. al. "Development of High-Performance, High-Volume Consumer MEMS Gyroscopes." *Solid-State Sensor, Actuator and Microsystems Workshop, Hilton Head Island.* 2010.

Micromechanical Gyroscopes

- Example: The Tuning Fork Gyroscope (TFG)

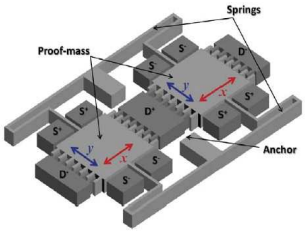

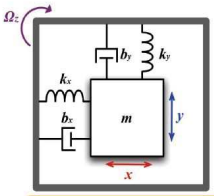

Lumped-Element Model

- Equations of motion of an ideal gyroscope:

Mode 1

$$m\frac{\partial^2 x}{\partial t^2}+b_x\frac{\partial x}{\partial t}+k_x x = F_{elecx}+2m\lambda\Omega_Z\frac{\partial y}{\partial t}$$

Mode 2

$$m\frac{\partial^2 y}{\partial t^2}+b_y\frac{\partial y}{\partial t}+k_y y = F_{elecy}-2m\lambda\Omega_Z\frac{\partial x}{\partial t}$$

Modes of Operation

Rotation-Rate Gyros

- Output proportional to Ω

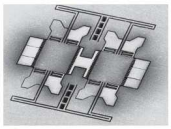

- Mode 1 driven into oscillation
- Mode 2 used to detect rotation

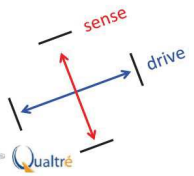

Whole-Angle Mode Gyros

- Output proportional to θ

- Free-vibrating structure
- Standing-wave precesses

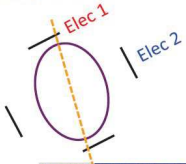

Electrostatic Transducers

Parallel-Plate Transducer

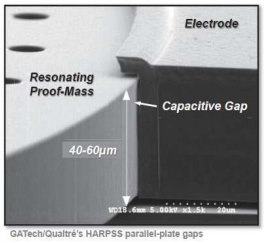

GATech/Qualtré's HARPSS parallel-plate gaps

- ✓ High electromechanical coupling
- ✓ Small and easy to implement
- ✗ Non-linear transfer function

$$\frac{dC}{dx}=\frac{\varepsilon\cdot w\cdot t}{(g_0-x)^2}\approx\frac{\varepsilon\cdot w\cdot t}{g_0^2}$$

Comb-Drive Actuation

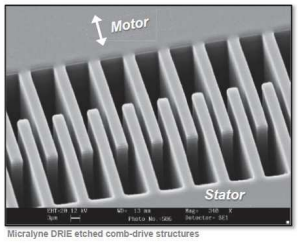

Micralyne DRIE etched comb-drive structures

- ✓ Linear actuation
- ✓ Allows large displacements
- ✗ Low coupling coefficient

$$\frac{dC}{dx}=\frac{\varepsilon\cdot 2n\cdot t}{g_0}$$

Mode-Split vs. Mode-Matched Gyros

Mode-Split Gyros

- Typically of Tuning-Fork kind

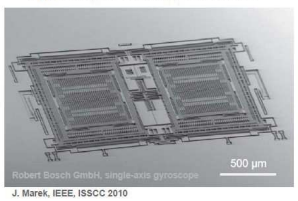

J. Marek, IEEE, ISSCC 2010

- Modes from different mechanisms
- Large BW (accelerometer response)
- Scale factor ∝ $1/\omega^2_{sns}$
  - Large mass (bigger size)
  - Low spring constant (poor reliability)

Mode-Matched Gyros

- Typically axisymmetric

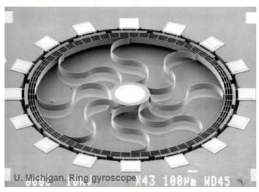

U. Michigan, Ring gyroscope

- Inherent degenerate modes
- BW proportional to f_0/Q
- Scale factor ∝ Q
  - 10,000 to 1'000,000 larger!!

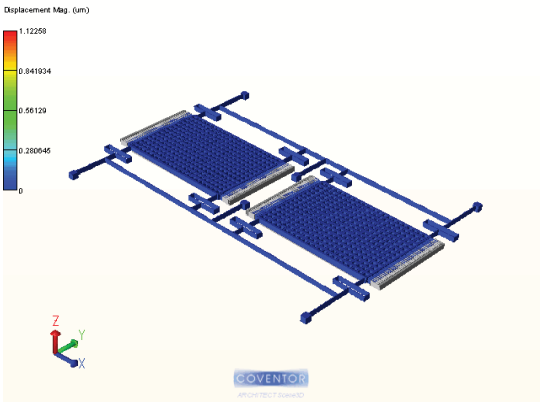

https://www.coventor.com/products/coventormp/mems-plus/visualization/

Gyroscope Application Example: Segway

- Silicon Sensing Systems VSG ring sensor "Dynamic Stabilization"
- Five sensors used to monitor orientation of the scooter, sampled at 100 times/second. Sensors include VSG ring gyroscopes and liquid-filled tilt sensors

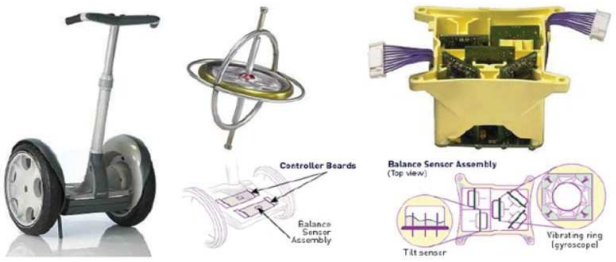

MEMS gyroskopy

INS – Intertial Navigation System

IMU (Inertial Measurement Unit)
– len senzory a data

AHRS (Attitude and Heading Reference System)
– spracovanie, poskytuje attitude including roll, yaw and pitch.

Sensor fusion: drift from the gyroscopes integration is compensated for by reference vectors, namely gravity, and the earth magnetic field (*Mahony*, *Madgwick* and *NXP Sensor Fusion*)

Extended Kalman filter

IMU – Inertial measurement unit

Racelogic's Inertial Measurement Unit (RLVBIMU04)

VN-100 Rugged Inertial Measurement Unit and Attitude Heading Reference System (IMU/AHRS)

MEMSIC Inertial Measurement Units (IMU) IMU440CA-200/400

IMU – Inertial measurement unit

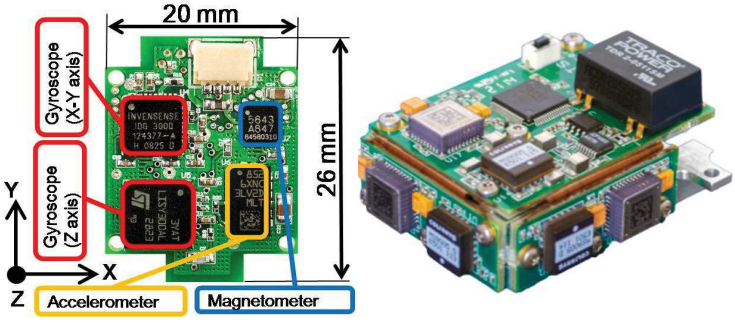

IMU – Inertial measurement unit

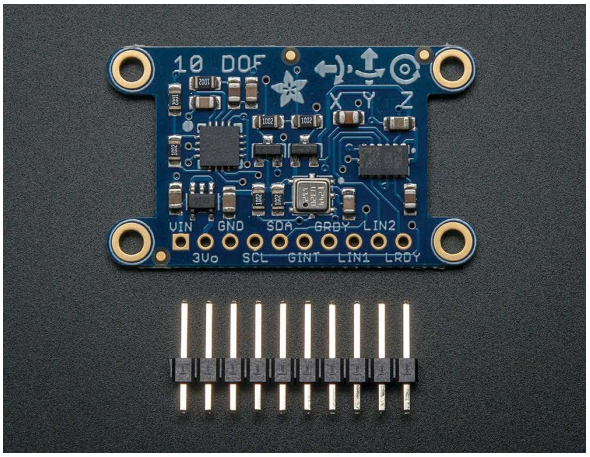

IMU – Inertial measurement unit

LSM303DLHC
3-axis accelerometer (up to +/-16g)
3-axis magnetometer (up to +/-8.1 gauss)

L3GD20
3-axis gyroscope (up to +/-2000 dps)

BMP180
barometric pressure sensor (300..1100 hPa)

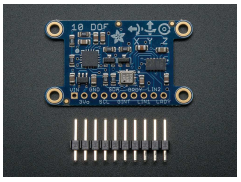

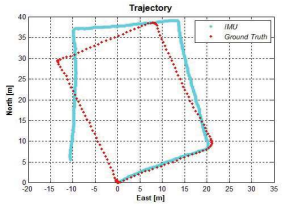

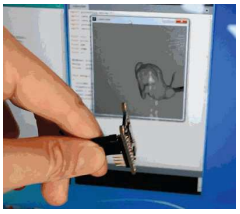

Multiaxis Inertial Measurement Unit (IMU)

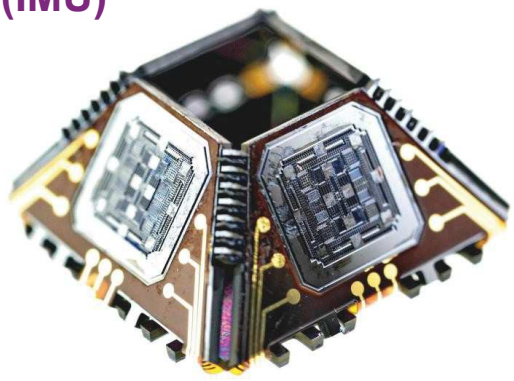

Multiaxis inertial measurement unit (IMU) created using a folded MEMS approach. The technology is expected to enable miniature systems for high-performance inertial navigation and guidance.

Photo by: Alexander Trusov

Inertial Measurement Unit (IMU)

https://www.youtube.com/watch?v=TJIntyaSNqM

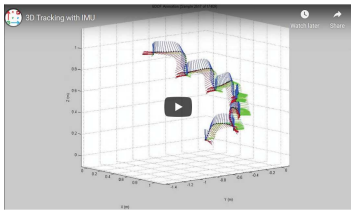

https://x-io.co.uk/gait-tracking-with-x-imu/

Cvičenia

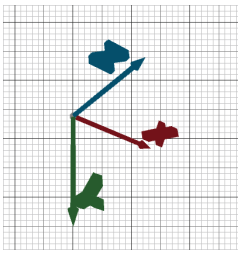

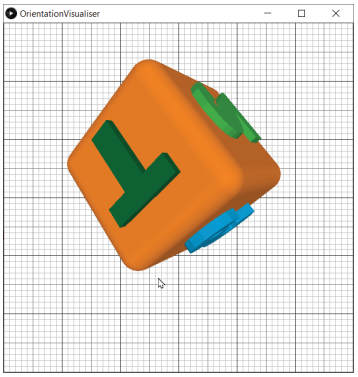

Cvičenia

Priečny náklon roll
Pozdĺžny sklon pitch
Zatáčanie yaw

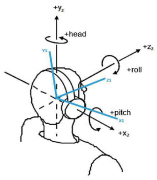

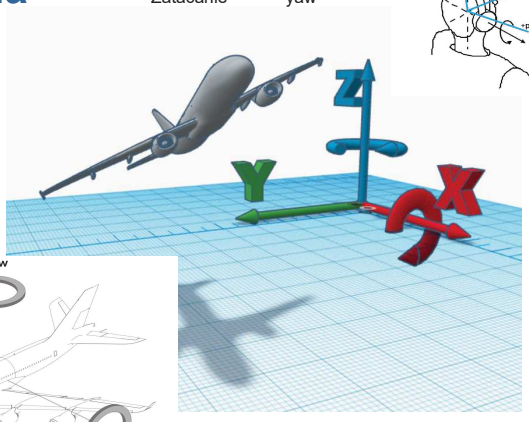

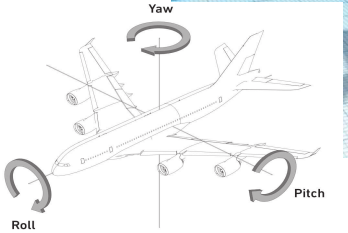

Cvičenia

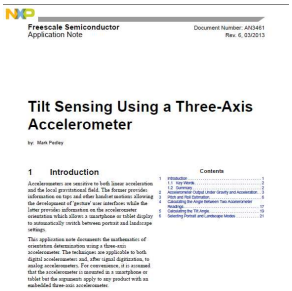

$$\tan\phi_{xyz} = \left(\frac{G_{py}}{G_{pz}}\right) \qquad \textit{Eqn. 25}$$

$$\tan\theta_{xyz} = \left(\frac{-G_{px}}{G_{py}\sin\phi + G_{pz}\cos\phi}\right) = \frac{-G_{px}}{\sqrt{G_{py}^{\,2} + G_{pz}^{\,2}}} \qquad \textit{Eqn. 26}$$